Self-assembled graphitic nanotubes with one-handed helical arrays of a chiral amphiphilic molecular graphene

Wusong Jin*, Takanori Fukushima*†, Makiko Niki*, Atsuko Kosaka*, Noriyuki Ishii‡, and Takuzo Aida*†§

*Aida Nanospace Project, Exploratory Research for Advanced Technology, Japan Science and Technology Agency, National Museum of Emerging Science and Innovation, 2-41 Aomi, Koto-ku, Tokyo 135-0064, Japan; ‡Biological Information Research Center, National Institute of Advanced Industrial Science and Technology, Tsukuba Central-6, 1-1-1 Higashi, Tsukuba, Ibaraki 305-8566, Japan; and §Department of Chemistry and Biotechnology, School of Engineering, University of Tokyo, 7-3-1 Hongo, Bunkyo-ku, Tokyo 113-8656, Japan

Edited by Ryoji Noyori, RIKEN (The Institute of Physical and Chemical Research), Saitama, Japan, and approved June 17, 2005 (received for review February 1, 2005)

Self-assembly of a Gemini-shaped, chiral amphiphilic hexa-*peri*-hexabenzocoronene having two chiral oxyalkylene side chains, along with two lipophilic side chains, yields graphitic nanotubes with one-handed helical chirality. The nanotubes are characterized by an extremely high aspect ratio of >1,000 and have a uniform diameter of 20 nm and a wall thickness of 3 nm. The nanotubes with right- and left-handed helical senses were obtained from the (*S*)- and (*R*)-enantiomers of the amphiphile, respectively, due to an efficient translation of point chirality into supramolecular helical chirality. The (*S*)- and (*R*)-enantiomers coassemble at varying mole ratios to give nanotubes, whose circular dichroism profiles are almost unchanged over a wide range of the enantiomeric excess of the amphiphile (100–20%). The high level of chirality amplification thus observed indicates a long-range cooperativity in the self-assembling process. In sharp contrast, a hexabenzocoronene amphiphile with chiral lipophilic side chains did not form nanotubular assemblies. The present work demonstrates the majority rule in noncovalent systems and also may provide a synthetic strategy toward realization of molecular solenoids.

chirality | self-assembly

Helicity is one of the most essential structural elements for certain biomolecules such as peptides and DNA. The prominent functions of these biological components have motivated chemists to design artificial helical architectures (1–8), which can be used for a variety of applications such as chiral separation (9, 10) and sensing (11–15), asymmetric synthesis (16), liquid crystals (17–19), nonlinear optics (20, 21), and so forth. Recently, a hot issue of chirality has emerged in relation to the helicity of the hexagonal carbon lattice in carbon nanotubes, because it determines the conductive properties of carbon nanotubes (22–24). Conductive polymers with helical architectures (25) also have attracted attention in view of the concept of molecular solenoids (26, 27), although this concept has yet been a dream of scientists, because there are no molecular objects that fulfill certain requisites for conductivity and helicity. Here, we report an example of conductive tubular objects consisting of one-handed helical arrays of a π-stacked chiral molecular graphene. Self-assembly of hexa-*peri*-hexabenzocoronene (HBC) derivatives to form discotic liquid crystals and nanofibers has been studied extensively by Müllen and coworkers (28, 29). We recently found that an amphiphilic HBC derivative (**1**) (Fig. 1) self-assembles in polar organic solvents such as tetrahydrofuran (THF) to give graphitic nanotubes, whose wall consists of a bilayer tape formed from bilaterally coupled columns of π-stacked HBC units (30). In the course of this work, we have noticed that the self-assembly of **1**, although achiral, gives a mixture of coiled and tubular assemblies under certain conditions, suggesting that the tubular objects also bear a helical structural element. This observation prompted us to design chiral HBC amphiphiles **2** and **3** (Fig. 1) that may lead to one-handed helical graphitic nanotubes. In the present work, we describe the synthesis and self-assembling behaviors of these chiral HBC amphiphiles and characterization of the resulting self-assembled structures, with an emphasis on the translation of point chirality into supramolecular helical chirality. We also highlight a chiral amplification phenomenon in the self-assembling event.

Materials and Methods

Synthesis of Chiral HBC Amphiphile 2. A $MeNO_2$ (7 ml) solution of anhydrous $FeCl_3$ (1.56 g, 9.60 mmol) was slowly added to a dry CH_2Cl_2 (70 ml) solution of 2,3-bis[4′-(2*S*)-{2-[2-(2-methoxyethoxy)ethoxy]propoxy}-4-biphenylyl]-5,6-di(4-dodecylpheny)-1,4-diphenylbenzene (440 mg, 0.32 mmol) (see *Supporting Materials and Methods*, which is published as supporting information on the PNAS web site) under bubbling with Ar through a glass capillary. After being stirred for 1 h, the reaction mixture was poured into MeOH (300 ml). The resulting yellow precipitate was isolated by filtration and subjected to column chromatography (SiO_2, hot THF), followed by size-exclusion chromatography (Bio-Rad BioBeads S-X1, CH_2Cl_2), and a fraction containing the target molecule was isolated and subjected to precipitation from 2-methyltetrahydrofuran (MeTHF) to give (*S*)-**2** as yellow sticky solid in 80% yield (350 mg). Likewise, enantiomeric counterpart (*R*)-**2** was obtained in 74% yield. ^{1}H NMR (500 MHz, THF-d_8) δ 8.46 (s, 2H), 8.34 (s, 2H), 8.18 (d, J = 8.5 Hz, 2H), 8.07 (d, J = 9.0 Hz, 2H), 7.94 (s, 2H), 7.92 (s, 2H), 7.75 (d, J = 8.0 Hz, 4H), 7.32 (t, J = 7.5 Hz, 2H), 7.16 (d, J = 8.5 Hz, 4H), 4.23–4.20 (m, 2H), 4.05–3.99 (m, 4H), 3.85–3.83 (m, 4H), 3.70–3.66 (m, 8H), 3.55–3.51 (m, 4H), 3.35 (s, 6H), 2.79 (t, J = 8.5 Hz, 4H), 1.82–1.81 (m, 4H), 1.55–1.24 (m, 42H), 0.86 (t, J = 7.0 Hz, 6H). ^{13}C NMR (125 MHz, THF-d_8): δ 158.78, 139.14, 136.69, 134.05, 129.33, 128.94, 128.45, 124.86, 123.88, 122.75, 121.99, 120.45, 118.90, 118.70, 118.63, 118.57, 114.87, 74.55, 72.20, 72.01, 71.15, 70.71, 69.19, 58.22, 37.09, 32.23, 32.12, 30.25, 30.14, 30.09, 30.03, 29.94, 29.61, 22.80, 17.29, 13.69. MALDI-TOF-MS: calculated for $C_{94}H_{104}O_8$ $[M + H]^+$: m/z = 1363.84; found: 1,363.84.

Synthesis of Chiral HBC Amphiphile 3. A $MeNO_2$ (30 ml) solution of anhydrous $FeCl_3$ (3.80 g, 23.2 mmol) was slowly added to a dry CH_2Cl_2 (150 ml) solution of 2,3-bis[4-(*S*)-(3,7-dimethyloctyl)-phenyl]-5,6-bis(4′-{2-[2-(2-methoxyethoxy)ethoxy]ethoxy}-4-

This paper was submitted directly (Track II) to the PNAS office.

Abbreviations: HBC, hexa-*peri*-hexabenzocoronene; TEM, transmission EM; THF, tetrahydrofuran; MeTHF, 2-methyltetrahydrofuran.

†To whom correspondence may be addressed. E-mail: aida@macro.t.u-tokyo.ac.jp or fukushima@nanospace.miraikan.jst.go.jp.

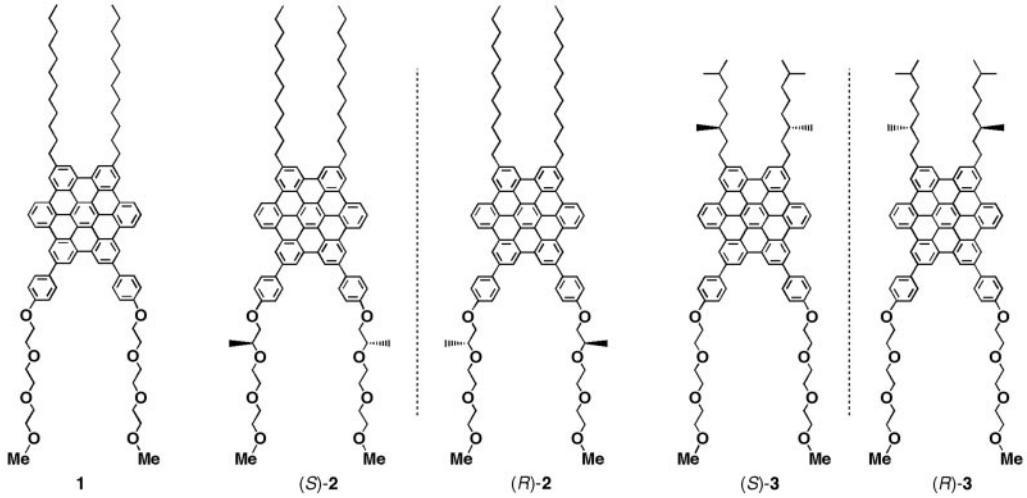

Fig. 1. Molecular structures of HBC amphiphiles **1**–**3**.

biphenylyl)-1,4-diphenylbenzene (1.00 g, 0.77 mmol) (see *Supporting Materials and Methods*) under bubbling with Ar through a glass capillary. After being stirred for 1 h, the reaction mixture was poured into MeOH (300 ml). The resulting yellow precipitate was isolated by filtration and subjected to column chromatography (SiO_2, hot THF), followed by size-exclusion chromatography (Bio-Rad BioBeads S-X1, CH_2Cl_2), and a fraction containing the target molecule was isolated and subjected to precipitation from THF to give (*S*)-**3** as yellow solid in 66% yield (630 mg). ^{1}H NMR (500 MHz, THF-d_8): δ 8.37 (s, 2H), 8.25 (s, 2H), 8.09 (d, J = 7.5 Hz, 2H), 8.00 (d, J = 6.5 Hz, 2H), 7.90 (s, 2H), 7.86 (s, 2H), 7.69 (d, J = 8.0 Hz, 4H), 7.25 (t, J = 7.0 Hz, 2H), 7.12 (d, J = 8.0 Hz, 4H), 4.28 (m, 4H), 3.99–3.97 (m, 4H), 3.80–3.78 (m, 4H), 3.73–3.71 (m, 4H), 3.68–3.66 (m, 4H), 3.55–3.54 (m, 4H), 3.35 (s, 6H), 2.82–2.74 (m, 4H), 1.83–1.81 (m, 4H), 1.65–1.24 (m, 18H), 1.13 (d, J = 6.5 Hz, 6H), 0.94 (d, J = 7.0 Hz, 12H). ^{13}C NMR (125 MHz, THF-d_8): δ 158.83, 136.85, 136.80, 136.56, 134.31, 133.96, 132.12, 129.42, 129.37, 129.04, 128.47, 122.14, 122.05, 120.67, 120.60, 118.95, 118.85, 118.77, 118.71, 114.87, 72.19, 71.02, 70.89, 70.67, 69.95, 67.79, 58.19, 39.87, 39.68, 37.61, 34.72, 33.42, 28.25, 25.18, 22.45, 22.33, 19.53. MALDI-TOF-MS: calculated for $C_{88}H_{94}O_8$ $[M]^+$: m/z = 1,278.68; found: 1,278.73.

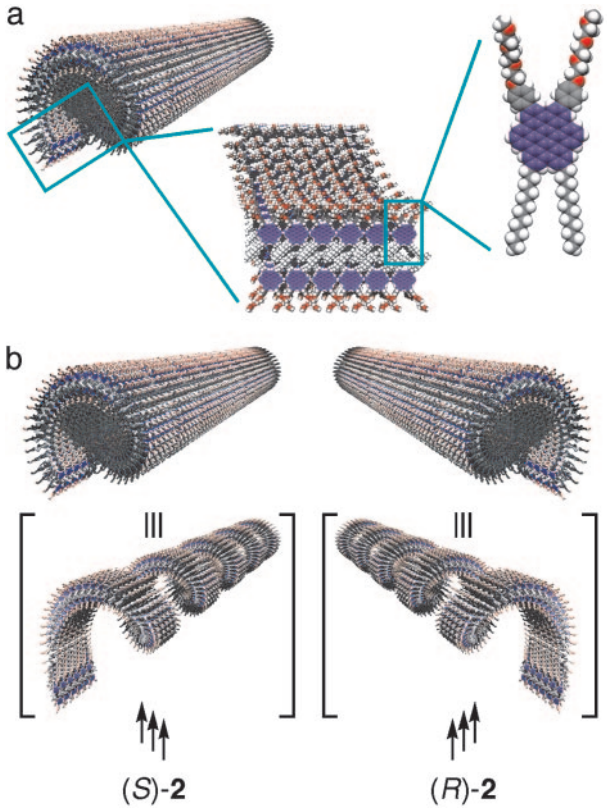

Fig. 2. Formation of the self-assembled graphitic nanotubes. (*a*) Schematic illustrations of the structure of self-assembled graphitic nanotube consisting of HBC amphiphile **1**. (*b*) Formation of chiral graphitic nanotubes with one-handed helical arrays of π-stacked HBC units through translation of point chirality into supramolecular helical chirality.

Results and Discussion

Molecular Design of Chiral HBC Amphiphiles. Our synthetic strategy toward self-assembled graphitic nanotubes makes use of a Gemini-shaped nonionic HBC amphiphile (**1**) bearing two paraffinic long alkyl chains on one side and two triethylene glycol (TEG) chains on the other (30). Self-assembly of **1** in THF gives a highly crystalline bilayer tape, consisting of two graphitic layers of

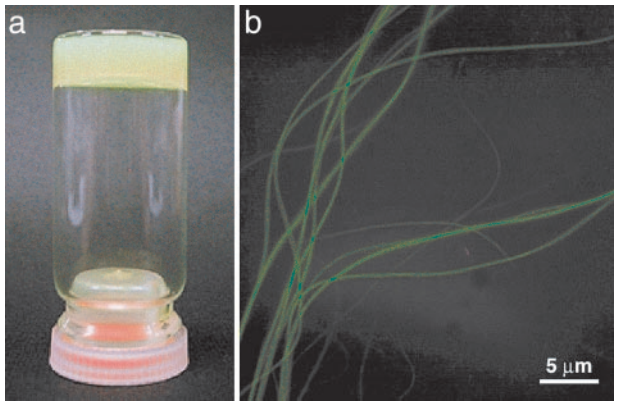

Fig. 3. Self-assembly of chiral HBC amphiphile **2**. (*a*) A gelatinous suspension formed at 20°C upon slow cooling of a hot MeTHF solution of chiral HBC amphiphile (*S*)-**2** (3 mg/ml). (*b*) Fluorescence micrograph of fibers formed at 20°C upon slow cooling of a hot MeTHF solution of (*S*)-**2** (1 mg/ml). A droplet of the suspension was sandwiched by glass plates and exposed to UV light.

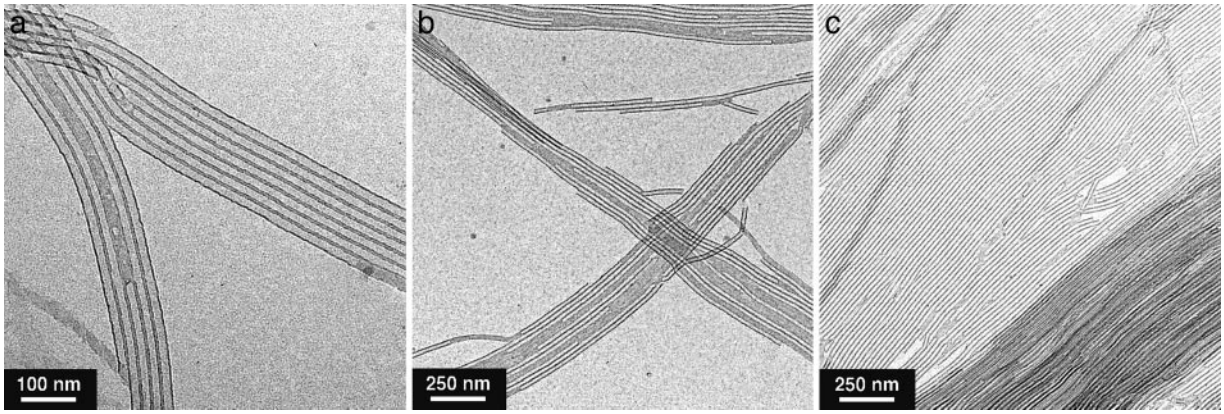

Fig. 4. TEM micrographs of nanotubes formed from chiral HBC amphiphile (*S*)-**2** in MeTHF (*a*), ClCy (*b*), and MeTHF/MeOH (*c*). For the preparation of samples *a* and *b*, suspensions, formed by slow cooling of the hot solutions (1 mg/ml) from 50° to 20°C, were diluted by a factor of 10, applied onto a specimen grid covered with a thin carbon support film, and air-dried. For the preparation of sample *c*, a MeOH vapor was allowed to diffuse slowly into a dilute MeTHF solution at 20°C, and the resulting suspension was treated similarly to the above.

π-stacked HBC units, which are connected by interdigitation of the paraffinic side chains (Fig. 2*a*). Helical rolling-up of the bilayer tape results in an equimolar (racemic) mixture of right- and left-handed helical nanotubes, where the paraffinic side chains are located within the wall, while the hydrophilic TEG chains cover both the inner and outer surfaces of the nanotube. Based on these observations, we anticipated that incorporation of a stereogenic center into the hydrophobic or hydrophilic side chains of **1** could give rise to a thermodynamic bias to either the right- or left-handed helical HBC array in the resulting nanotubular assembly. Thus, we synthesized chiral HBC amphiphiles **2** and **3** (Fig. 1), which bear a point chirality in the hydrophilic and hydrophobic side chains, respectively.

Structural Aspects of Self-Assembly of Chiral HBC Amphiphiles. Although chiral HBC amphiphile **2**, in contrast with achiral version **1** (30), was highly soluble in THF even at room temperature, MeTHF was found to be more suited for the controlled self-assembly of **2**. Thus, compound (*S*)-**2** was suspended in MeTHF (1 mg/ml) and heated to 50°C. When allowed to cool to 20°C, the resulting yellow-colored solution gradually turned cloudy within a few hours. When the concentration of (*S*)-**2** in MeTHF was higher (3 mg/ml), a gelatinous suspension resulted (Fig. 3*a*). Fluorescence microscopy of the suspension, after being cast on a glass substrate, showed the presence of several tens of micrometer-long fibers (Fig. 3*b*). Transmission EM (TEM) of an air-dried suspension (Fig. 4*a*) demonstrated that these fibers are tubular, having a uniform diameter of 20 nm with a wall thickness of 3 nm. Self-assembly of (*S*)-**2** in chlorocyclohexane (ClCy) also gave nanotubes with an analogous dimension (Fig. 4*b*). We also noticed that slow diffusion of a MeOH vapor at 20°C into a dilute MeTHF solution of (*S*)-**2** results in the

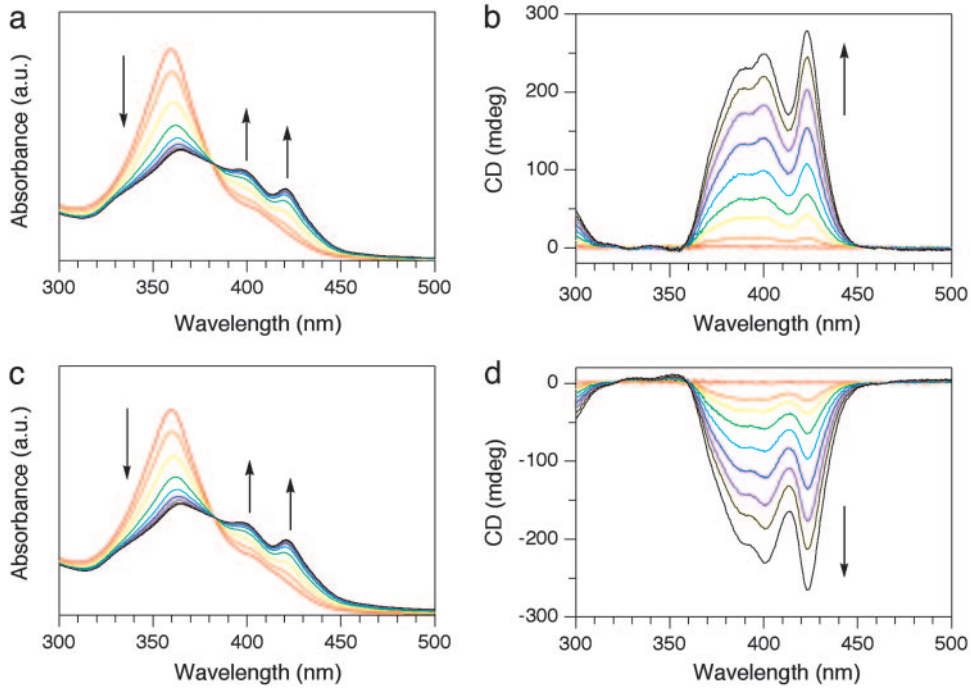

Fig. 5. Time-dependent changes in electronic absorption and CD spectra of the enantiomers of chiral HBC amphiphile (*S*)-**2** (*a* and *b*) and (*R*)-**2** (*c* and *d*) in MeTHF (3 mg/ml) at 20°C, on rapid cooling from 50°C in a quartz cell of 0.1-mm path length. The spectra were taken with a 3-min interval. a.u., arbitrary units.

formation of longer and highly aligned nanotubes (Fig. 4*c*). IR spectroscopy of tubularly assembled (*S*)-**2** on a KBr plate showed CH_2 stretching vibrations at 2,917 (ν_{anti}) and 2,849 cm^{-1} (ν_{sym}), indicating that the long alkyl chains are stretched to form a crystalline domain. Considering the wall thickness, as evaluated by the TEM micrographs (Fig. 4*a*), the wall of the nanotube involves a bilayer structure supported by the crystalline paraffinic side chains of the HBC amphiphile (Fig. 2*a*). These results are analogous to the assembling behaviors observed for achiral HBC amphiphile **1** (30). Thus, the chiral functionalization of the hydrophilic side chains does not impair the capability of **1** to form nanotubular assemblies.

In sharp contrast, chiral HBC amphiphile **3** bearing branched asymmetric centers in the paraffinic side chains hardly gave nanotubular assemblies. For example, cooling of a hot MeTHF solution of (*S*)-**3** resulted in the formation of a yellow-colored powdery precipitate, which did not show any defined mesostructures in scanning EM (see Fig. 9, which is published as supporting information on the PNAS web site). Similar results were obtained when (*S*)-**3** was treated in other solvents such as THF and ClCy. IR spectroscopy of the solid substances, thus obtained from (*S*)-**3** in these solvents, all displayed CH_2 stretching vibrations at 2,924 (ν_{anti}) and 2,869 cm^{-1} (ν_{sym}), indicating the absence of crystalline paraffinic domains. The failure of the nanotube formation from (*S*)-**3** is most likely because of its branched paraffinic side chains that prevent the formation of a bilayer tape.

Spectral Aspects of Self-Assembly of Chiral HBC Amphiphiles. The absorption spectral profile of well-behaved chiral HBC amphiphile **2** was quite similar to that of previously reported achiral version **1** (30). For example, a MeTHF solution of (*S*)-**2** (3 mg/ml) at 50°C showed an absorption band centered at 360 nm, characteristic of highly dispersed HBCs. When the solution was allowed to cool to 20°C, the resultant suspension displayed a decrease in intensity of this absorption band and an appearance of red-shifted absorption bands at 398 and 421 nm, characteristic of π-stacked HBC units (30, 31). The hot solution of (*S*)-**2**, when rapidly cooled to 20°C, showed a time-dependent spectral change with an isosbestic point at 382 nm, which subsided within 30 min (Fig. 5*a*). Although the solution of (*S*)-**2** at 50°C was silent in CD spectroscopy, cooling of the solution resulted in the appearance of positive CD bands at 389, 400, and 423 nm, which were gradually intensified with time (Fig. 5*b*). Contribution of linear dichroism to the observed spectrum, if any, is negligibly small, because the intensities of these three bands were all intact to the rotation of the sample by 90° in a plane normal to the incident light. Because only the red-shifted absorption bands are CD-active, it is obvious that the optical activity of the system is originating from the π-stacked HBC units in the nanotubular assembly. We confirmed that the CD spectral profile of the enantiomer (*R*)-**2** and its temperature dependence are perfect mirror images of those observed for (*S*)-**2** (Fig. 5 *c* and *d*). Analogous absorption and CD spectral profiles were observed when ClCy was used in place of MeTHF (see Fig. 10, which is published as supporting information on the PNAS web site). From these observations, tubularly assembled **2** most likely contains a helical molecular arrangement of the π-stacked HBC units, whose sense depends on the absolute configuration of the stereogenic centers in the hydrophilic side chains. Fortunately, we found that helical coils are formed along with the perfect nanotubes when the self-assembly of **2** is promoted by diffusion of a hexane vapor into its dilute ClCy solution. From arbitrarily selected TEM images, we confirmed that all of the helical coils formed from (*S*)-**2** are right-handed, whereas those from (*R*)-**2** are left-handed (Fig. 6; see also Fig. 11, which is published as supporting information on the PNAS web site). The helical coils are considered as the topological precursors for the nanotubes

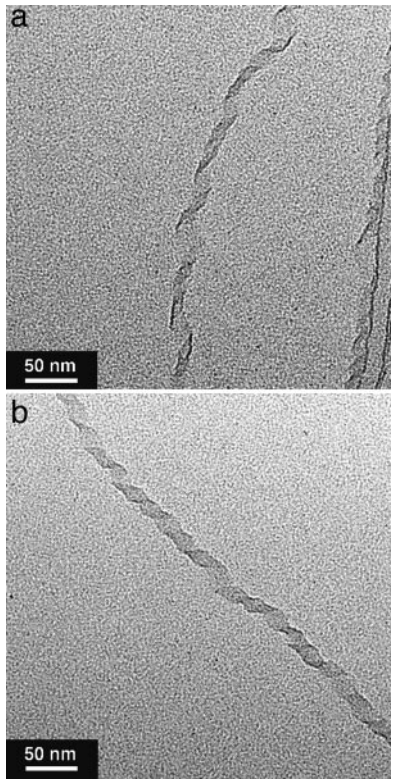

Fig. 6. TEM micrographs of self-assembled helical coils formed from the enantiomers of chiral HBC amphiphile (*S*)-**2** (*a*) and (*R*)-**2** (*b*). The samples were prepared by slow diffusion of a hexane vapor at 20°C into dilute ClCy solutions of **2**, applied onto a specimen grid covered with a thin carbon support film, and air-dried.

in the self-assembling event (Fig. 2*b*). As reported in ref. 30, the nanotubes from achiral HBC amphiphile **1** also contain such a helical structural element, but they are racemic. Conversely, the above results clearly demonstrate that use of chiral HBC amphiphile **2** gives rise to a large stereochemical bias in the self-assembling event toward either right- or left-handed helical array, leading to the optically active nanotubes (Fig. 2*b*).

In contrast with chiral HBC amphiphile **2**, ill-behaved chiral version (*S*)-**3**, which does not form nanotubular assemblies, displayed even at 50°C in MeTHF a poorly resolved, broad absorption band with maxima at 363, 415, and 440 nm. When this solution was rapidly cooled to 30°C, these characteristic absorption bands simply became less intensified with time (Fig. 7*a*), because (*S*)-**3** precipitated gradually as large aggregates. During this cooling event, the CD activity of the suspension remained very poor (Fig. 7*b*).

Chirality Amplification. Because the helical sense of the HBC nanotubes is determined by the absolute configuration of **2**, we investigated what would happen if the (*R*)- and (*S*)-enantiomers of **2** are allowed to coassemble under the conditions identical to those for the single enantiomers. At varying mole ratios of (*R*)- and (*S*)-**2** in MeTHF, perfect HBC nanotubes were formed, whose dimensions, as confirmed by TEM analysis, were virtually identical, although independent of the enantiomeric excess of **2** (see Fig. 12, which is published as supporting information on the PNAS web site). However, their thermal properties are slightly different from one another. In differential scanning calorimetry (DSC) (see Fig. 13, which is published as supporting information on the PNAS web site), the nanotubes from (*R*)- or (*S*)-**2** alone, on first heating, showed an intense endothermic peak at 140°C

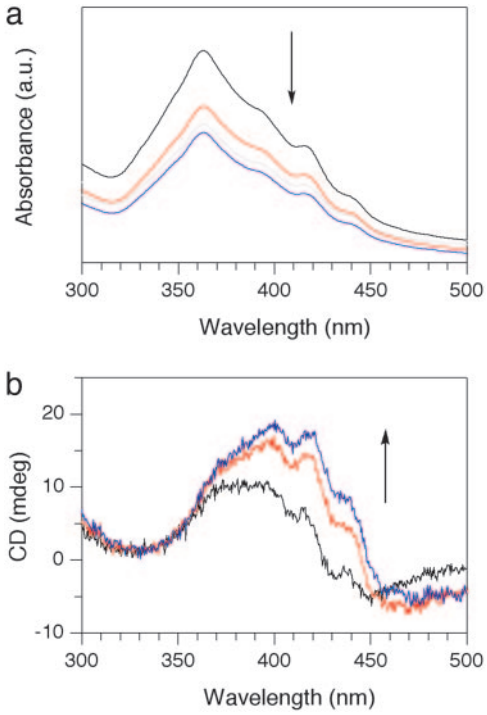

Fig. 7. Time-dependent changes in electronic absorption (*a*) and CD spectra (*b*) of chiral HBC amphiphile (*S*)-**3** in MeTHF (1 mg/ml) at 30°C on rapid cooling from 50°C in a quartz cell of 0.1-mm path length. The spectra were taken with a 3-min interval. a.u., arbitrary units.

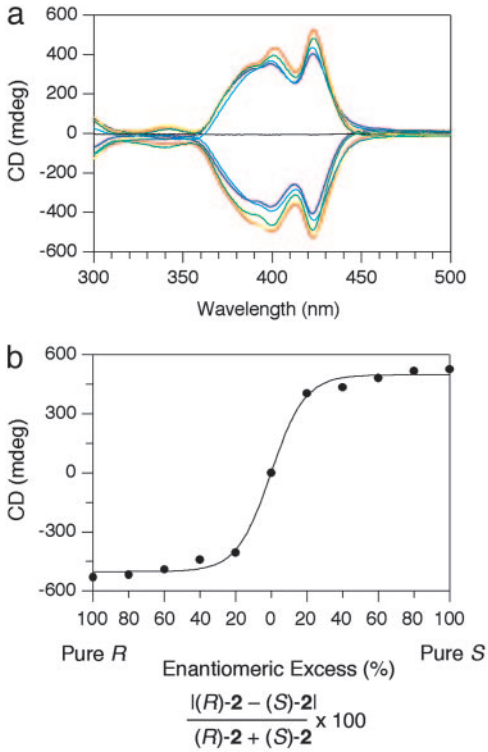

Fig. 8. Chirality amplification in the coassembly of (*R*)- and (*S*)-**2**. (*a*) CD spectra of self-assembled nanotubes formed from chiral HBC amphiphile **2** at varying mole ratios of its enantiomers in MeTHF (3 mg/ml) at 20°C, measured after 12 h upon cooling from 50°C. Enantiomeric excess = 100% (red), 80% (yellow), 60% (green), 40% (sky blue), 20% (blue), and 0% (black). (*b*) Change in intensity of the CD band at 423 nm.

and were transformed into a liquid crystalline mesophase through reorganization of the π-stacked HBC units (30). Conversely, when mixtures of (*R*)- and (*S*)-**2** were subjected to the self-assembling conditions, the endothermic DSC peak of the resulting nanotubes became a little broader and shifted toward the lower temperature range as the enantiomeric excess of **2** was lower. For example, the assembly of racemic **2** resulted in a phase transition temperature of 134°C. These results suggest that the (*R*)- and (*S*)-enantiomers of **2** coassemble with one another to form the nanotubes.

We investigated CD spectral features of the assembled mixtures of the (*R*)- and (*S*)-enantiomers of **2**. Thus, both enantiomers were mixed in MeTHF at a molar ratio (*R*)-**2** to (*S*)-**2** of 60:40 (20% enantiomeric excess), and the resulting suspension was heated at 50°C and then allowed to stand at 20°C. Quite interestingly, the CD spectrum of the suspension, measured after 2 weeks, was substantially identical to that observed for the case with (*R*)-**2** alone. Because the yield of the nanotubes after filtration was 93%, the observed CD profile is not the consequence of preferential self-assembly of major enantiomer (*R*)-**2** but the result of the coassembly of (*R*)- and (*S*)-**2**. Even though the enantiomeric excess of the chiral amphiphile was changed over a wide range from 20% to 100%, the CD spectrum of the suspension remained almost unchanged (Fig. 8*a*), resulting in a sigmoidal response of the CD intensity to the optical purity of **2** (Fig. 8*b*). The chiroptical profiles also suggest the absence of enantiomerically enriched domains in the helical nanotubes. Such a nonlinear phenomenon is referred to as "chirality amplification," where the major enantiomer incorporated into each nanotube determines the helical sense (majority rule) (1, 15, 32, 33).

The majority-rule principle has been studied extensively for covalently bonded helical polymers both from experimental and theoretical viewpoints (34–36). However, to our knowledge, examples of chirality amplification governed by the majority rule have never been reported for noncovalent, supramolecular polymers and assemblies (37, 38). According to the theory, the strength of chirality amplification depends on the free-energy penalty of a mismatch between the preferred helical handedness of a monomer and actual helical sense of the assembly compared with the energetic penalty for a helical sense reversal (33). Even though the mismatch penalty is large, a wrong enantiomer may still obey the majority when the energetic penalty of the helical sense reversal is much larger. Conversely, even though the mismatch penalty is small, a wrong enantiomer may form helical arrays of its own preference when the helical sense reversal is energetically much easier. As already described, the two enantiomers of **2** coassemble to form the nanotubes. Because the thermal properties of the nanotubes depend on the enantiomeric excess of the monomer (Fig. 13), the mismatch penalty certainly exists in this system. However, the occurrence of chirality amplification (Fig. 8) indicates that the energetic penalty for the helical sense reversal is much larger than the mismatch penalty. Also, from a morphological point of view, the helical sense reversal is not appropriate, because the formation of a coiled precursor, capable of rolling up to form the tubular assembly (Fig. 2*b*), cannot be expected.

Conclusions

We have demonstrated that graphitic nanotubes with right- and left-handed helical senses can be prepared, respectively, from the enantiomers of Gemini-shaped chiral HBC amphiphile (*S*)- and (*R*)-**2**, where the point chirality incorporated into the hydrophilic side chains of the HBC amphiphile is successfully translated into the supramolecular helical chirality of the resulting nanotubular assembly (Fig. 2*b*). In contrast, the

self-assembly of chiral HBC amphiphile **3** having stereogenic centers at the paraffinic side chains does not form nanotubes but irregular aggregates. The enantiomers of **2** coassemble to form nanotubes, whose helical sense is determined by the major enantiomer incorporated. Although such a chirality amplification phenomenon based on the majority rule is well known for covalent helical polymers, this phenomenon is unprecedented in supramolecular systems and would lead to a new area of chirotechnology. In particular, electrical conduction of the graphitic nanotubes with one-handed helical chirality is a highly interesting subject, as it may realize the concept of molecular solenoids.

Note. A Dutch group (38) independently reported a similar chirality amplification phenomenon in supramolecular systems while this work was under review.

1. Green, M. M., Meijer, E. W. & Nolte, R. J. M., eds. (2003) *Materials–Chirality*, Topics in Stereochemistry (Wiley Interscience, Hoboken, NJ), Vol. 24.
2. Hill, D. J., Mio, M. J., Prince, R. B., Hughes, T. S. & Moore, J. S. (2001) *Chem. Rev.* **101,** 3893–4011.
3. Cornelissen, J. J. L. M., Rowan, A. E., Nolte, R. J. M. & Sommerdijk, N. A. J. M. (2001) *Chem. Rev.* **101,** 4039–4070.
4. Nakano, T. & Okamoto, Y. (2001) *Chem. Rev.* **101,** 4013–4038.
5. Green, M. M., Cheon, K.-S., Yang, S.-Y., Park, J.-W., Swansburg, S. & Liu, W. (2001) *Acc. Chem. Res.* **34,** 672–680.
6. Hirschberg, J. H. K., Brunsveld, L., Ramzl, A., Vekemans, J. A. J. M., Sijbesma, R. P. & Meijer, E. W. (2000) *Nature* **407,** 167–170.
7. Fenniri, H., Mathivanan, P., Vidale, K. L., Sherman, D. M., Hallenga, K., Wood, K. V. & Stowell, J. G. (2001) *J. Am. Chem. Soc.* **123,** 3854–3855.
8. Percec, V., Dulcey, A. E., Balagurusamy, V. S. K., Miura, Y., Smidrkal, J., Peterca, M., Nummelin, S., Edlund, U., Hudson, S. D., Heiney, P. A., *et al.* (2004) *Nature* **430,** 764–768.
9. Okamoto, Y. & Yashima, E. (1998) *Angew. Chem. Int. Ed.* **37,** 1020–1043.
10. Guo, Y.-M., Oike, H., Saeki, N. & Aida, T. (2004) *Angew. Chem. Int. Ed.* **43,** 4915–4918.
11. Tanatani, A., Mio, M. & Moore, J. S. (2001) *J. Am. Chem. Soc.* **123,** 1792–1793.
12. Fenniri, H., Deng, B.-L. & Ribbe, A. E. (2002) *J. Am. Chem. Soc.* **124,** 11064–11072.
13. Nonokawa, R. & Yashima, E. (2003) *J. Am. Chem. Soc.* **125,** 1278–1283.
14. Guo, Y.-M., Oike, H. & Aida, T. (2004) *J. Am. Chem. Soc.* **126,** 716–717.
15. Yashima, E., Maeda, K. & Nishimura, T. (2004) *Chem. Eur. J.* **10,** 42–51.
16. Feringa, B. L. & van Delden, R. A. (1999) *Angew. Chem. Int. Ed.* **38,** 3418–3438.
17. Goodby, J. W. (1998) in *Handbook of Liquid Crystals: Fundamentals*, eds. Demus, D., Goodby, J., Gray, G. W., Spiess, H.-W. & Vill, V. (Wiley, Weinheim, Germany), Vol. 1, pp. 115–132.
18. Green, M. M., Zanella, S., Gu, H., Sato, T., Gottarelli, G., Jha, S. K., Spada, G. P., Schoevaars, A. M., Feringa, B. & Teramoto, A. (1998) *J. Am. Chem. Soc.* **120,** 9810–9817.
19. Oda, M., Nothofer, H.-G., Lieser, G., Scherf, U., Meskers, S. C. J. & Neher, D. (2000) *Adv. Mater.* **12,** 362–365.
20. Kauranen, M., Veerbiest, T., Bouttoon, C., Teerenstra, M. N., Clays, K., Schouten, A. J., Nolte, R. J. M. & Persoons, A. (1995) *Science* **270,** 966–969.
21. Verbiest, T., Van Elshocht, S., Kauranen, M., Hellemans, L., Snauwaert, J., Nuckolls, C., Katz, T. J. & Persoons, A. (1998) *Science* **282,** 913–915.
22. Wildöer, J. W. G., Venema, L. C., Rinzler, A. G., Smalley, R. E. & Dekker, C. (1998) *Nature* **391,** 59–62.
23. Odom, T. W., Huang, J.-L., Kim, P. & Lieber, C. M. (1998) *Nature* **391,** 62–64.
24. Dresselhaus, M. S., Dresselhaus, G. & Avouris, P., eds. (2001) *Carbon Nanotubes: Synthesis*, *Structure*, *Properties and Applications* (Springer, Berlin).
25. Akagi, K., Piao, G., Kaneko, S., Sakamaki, K., Shirakawa, H. & Kyotani, M. (1998) *Science* **282,** 1683–1686.
26. Akagi, K., Piao, G., Kaneko, S., Higuchi, I., Shirakawa, H. & Kyotani, M. (1999) *Synth. Metals* **102,** 1406–1409.
27. Tagami, K., Tsukada, Y., Wada, Y., Iwasaki, T. & Nishide, H. (2003) *J. Chem. Phys.* **119,** 7491–7497.
28. Simpson, C. D., Wu, J., Watson, M. D. & Müllen, K. (2004) *J. Mater. Chem.* **14,** 494–504.
29. Watson, M. D., Fechtenkötter, A. & Müllen, K. (2001) *Chem. Rev.* **101,** 1267–1300.
30. Hill, J. P., Jin, W., Kosaka, A., Fukushima, T., Ichihara, H., Shimomura, T., Ito, K., Hashizume, T., Ishii, N. & Aida, T. (2004) *Science* **304,** 1481–1483.
31. Fleming, A. J., Coleman, J. N., Dalton, A. B., Fechtenkötter, A., Watson, M. D., Müllen, K., Byrne, H. J. & Blau, W. J. (2003) *J. Phys. Chem. B* **107,** 37–43.
32. Green, M. M., Park, J.-W., Sato, T., Teramoto, A., Lifson, S., Selinger, R. L. B. & Selinger, J. V. (1999) *Angew. Chem. Int. Ed.* **38,** 3138–3154.
33. Green, M. M. (2000) in *Circular Dichroism: Principles and Applications*, eds. Berova, N., Nakanishi, K. & Woody, R. W. (Wiley–VCH, New York), 2nd Ed., pp. 491–520.
34. Green, M. M., Peterson, N. C., Sato, T., Teramoto, A., Cook, R. & Lifson, S. (1995) *Science* **268,** 1860–1866.
35. Green, M. M., Garetz, B. A., Munoz, B. & Chang, H. (1995) *J. Am. Chem. Soc.* **117,** 4181–4182.
36. Tang, K., Green, M. M., Cheon, K. S., Selinger, J. V. & Garetz, B. A. (2003) *J. Am. Chem. Soc.* **125,** 7313–7323.
37. van Gestel, J. (2004) *Macromolecules* **37,** 3894–3898.
38. van Gestel, J., Palmans, A. R. A., Titulaer, B., Vekemans, J. A. J. M. & Meijer, E. W. (2005) *J. Am. Chem. Soc.* **127,** 5490–5494.